Supplementary file - BioPathNet: Enhancing Link Prediction in Biomedical Knowledge Graphs through Path Representation Learning

Yue Hu[1,2,+*], Svitlana Oleshko[1,5,+], Samuele Firmani[1,+], Zhaocheng Zhu[3,4], Hui Cheng[5], Maria Ulmer[1,2], Matthias Arnold[1,2], Maria Colomé-Tatché[1,2,6], Jian Tang[3,7,8], Sophie Xhonneux[3,4,§], Annalisa Marsico[1,§*]

[+]equal contribution.
[§]co-last author.

[1]Computational Health Center, Helmholtz Center Munich, Ingolstaedter Landstrasse 1, Neuherberg, 85764, Bavaria, Germany.
[2]School of Life Sciences, Technical University of Munich, Alte Akademie 8, Freising, 85354, Bavaria, Germany.
[3]Department, Mila - Québec AI Institute, 6666 St-Urbain, Montréal, QC H2S 3H1, Quebec, Canada.
[4]Department, Université de Montréal, 2900, boul. Édouard-Montpetit, Montréal, QC H3T 1J4, Quebec, Canada.
[5]School of Computation, Information and Technology, Technical University of Munich, Arcisstrasse 21, Munich, 80333, Bavaria, Germany.
[6]Faculty of Biology, Ludwig-Maximilians University, Grosshaderner Str. 2, Planegg-Martinsried, 82152, Bavaria, Germany.
[7]Department, CIFAR AI Chair, 661 University Ave, Toronto, ON M5G 1M1, Ontario, Canada.
[8]Department, HEC Montréal, 3000 Chem. de la Côte-Sainte-Catherine, Montréal, QC H3T 2A7, Quebec, Canada.

*Corresponding author(s). E-mail(s): yue.hu@helmholtz-munich.de; annalisa.marsico@helmholtz-munich.de;
Contributing authors: svitlana.oleshko@helmholtz-munich.de; samuele.firmani@helmholtz-munich.de; zhaocheng.zhu@umontreal.ca; hui.cheng@helmholtz-munich.de; maria.colometatche@helmholtz-munich.de; jian.tang@hec.ca; sophie.xhonneux@mila.quebec;

Keywords: biomedical knowledge graph, link prediction, graph neural network

Contents

1 Extended Methods

1.1 Neural Bellman-Ford Network (NBFNet)

Our newly developed BioPathNet is a path-representation learning-based method for graph completion built upon the NBFNet framework. Below, we describe the foundations of NBFNet to provide an understanding of how BioPathNet operates.

Unlike node embedding methods or node GNN encoders that infer links between entities in a KG by learning node representations in an embedding space, NBFNet is a general graph neural network framework that performs link prediction by learning representations for each path from the query entity to potential tail entities. This is done by considering the relations along each possible path between the query entity and the potential tail entity. Given a KG, NBFNet learns to predict the tail node for a query $(u, q, ?)$. It does this by learning a node pair representation $h_q(u, v)$ for nodes u and v, which captures all the possible paths between u and v conditioned on q. In NBFNet, the path formulation is represented by a generalized sum of path representations between u and v, denoted by $h_q(P)$, with a commutative summation operator $\bigoplus$:

$$h_q(u, v) = h_q(P_1) \oplus h_q(P_2) \oplus ..... \oplus h_q(P_M) \tag{1}$$

where M denotes the possible number of paths between u and v. Each path representation $h_q(P)$ is defined as the generalized product of the edges (or edges representations) belonging to that path, with the multiplication operator $\bigotimes$.

$$h_q(P) = w_q(e_1) \otimes w_q(e_1) \otimes ..... \otimes w_q(e_p) \tag{2}$$

where p is number of edges $e_1, ..., e_p$ belonging to path P. In compact form, the path formulation can be written as:

$$h_q(u, v) = \bigoplus_{p \in P_{u,v}} \bigotimes_{e \in P} w_q(e) \tag{3}$$

This, in practice, means that we compute the representation between nodes u and v under query relation q by considering every path between the source node u and the target node v. Each path is represented by the product of edge representations w_q along that path, and we sum these products to obtain the final representation.

Two key factors contribute to NBFNet's scalability for large graphs and its effectiveness in learning tasks: the use of the generalized Bellman-Ford dynamic programming framework for path representation and the abstraction of this process into a neural formulation.

Generalized Bellmann-Ford path representation The approach above, which predicts a link between a head and tail node by enumerating all possible paths and summing their contributions, is not scalable. As the network grows, the number of possible paths between the head and tail nodes increases exponentially, making this method impractical for larger networks. To achieve a scalable path formulation, NBFNet utilizes the Bellman-Ford dynamic programming algorithm, which efficiently finds the shortest path from a single source node to all other nodes in a weighted graph through a recursive process [1]:

$$d[v] = min(d[u] + w(u, v)) \tag{4}$$

By extending this equation to generalize the addition operator to any summation operator $\bigoplus$ and the minimum operator to any multiplication operator $\bigotimes$, we derive the generalized Bellman-Ford algorithm [2]. This generalization transforms the original Bellman-Ford algorithm for shortest path calculation into a versatile framework that simultaneously computes pair representations $h_q(u, v)$ for a given entity u, query relation q, and all vertices v in a graph. This approach reduces the computational cost to polynomial time relative to the number of nodes and edges in the graph. The formulation of the generalized Bellman-Ford algorithm is as follows:

$$h_q^{(0)}(u,v) \leftarrow \mathbb{1}_q(u=v) \tag{5}$$

$$h_q^{(t)}(u,v) \leftarrow \Big(\bigoplus_{(x,v)\in\mathcal{E}} h_q^{(t-1)}(u,x) \otimes w_q(x,r,v)\Big) \oplus h_q^{(0)}(u,v) \tag{6}$$

It first initializes the boundary condition on the source node (equation 5), representing the shortest path between u and v at the start. If the head and tail nodes coincide ($u = v$), the boundary condition is set to the generalized $\mathbb{1}$, which corresponds to 0 in the shortest path context (i.e., the shortest distance between a node and itself is zero) and to ∞ in the case $u \neq v$. Equation 6 describes the Bellman-Ford iteration, updating the shortest path distance between u and v. In each iteration, the representation from the previous layer $(t-1)$ is multiplied by the transition edge representation w_q to obtain the new representation $h_q(u,v)$. Here, W_q is a function of the relation between u and v. The boundary condition is added at each step to ensure accurate path formulation. The algorithm starts by propagating the boundary condition from the source node to its neighbors. Thanks to the distributive properties of the multiplication operator, all prefixes sharing this propagation are computed simultaneously. This iterative process continues, assessing potential target nodes, until all paths from the source node to the tail node are covered after t iterations, where t represents the path length.

Neural formulation The generalized summation and multiplication operators are handcrafted. By abstracting the boundary condition in equation 5 to an indicator function, the multiplication operator in equation 6 to a message passing formulation, and the summation operator to a general aggregation function, NBFNet extends the generalized path formulation of the Bellman-Ford algorithm into a neural network framework. In this formulation, neural network functions parametrize the boundary condition, multiplication, and summation functions, allowing a generalized GNN framework to learn these three neural functions effectively.

$$h_v^{(0)} \leftarrow INDICATOR(u,v,q) \tag{7}$$

$$h_v^{(t)} \leftarrow AGGREGATE(\{MESSAGE(h_x^{(t-1)}, w_q(x,r,v)) | (x,r,v) \in \mathcal{E}(v)\} \cup \{h_v^{(0)}\}) \tag{8}$$

For the indicator function, NBFNet learns the embedding of the query relation q and assigns q to node v if v equals the source node u. For message passing, NBFNet borrows relational operators from KG embeddings, such as translation from TransE, multiplication from DistMult, and rotation from RotatE. Aggregation functions are implemented using permutation-invariant functions from GNN literature, including sum, mean, max, and principal neighborhood aggregation (PNA). Traditionally, edge representations are defined as transition probabilities or lengths. However, since an edge's contribution varies with the query relation, NBFNet parameterizes edge representations as a linear function of the query relation [3]. NBFNet can be interpreted as a novel GNN framework for learning pair representations. Unlike common GNN frameworks, which compute pair representations as two independent node representations $h_q(u)$ and $h_q(u)$, in NBFNet, each node learns a representation conditioned on the source node. The learned pair representation $h_q(u,v)$ is then used to solve the link prediction problem, i.e., predicting the tail entity v given the head entity u and relation q. This is formulated as the conditional likelihood of the tail entity v as:

$$p(v|u,q) = \sigma(f(h_q(u,v))) \tag{9}$$

where where $\sigma(\_)$ is the sigmoid function and $f(\_)$ is a feed-forward neural network.

1.2 Gene function prediction task

The following hyperparameters of BioPathNet were optimized for: adversarial temperature (corresponding to the temperature in self-adversarial negative sampling) $\{0.5, 1.0, 2.0\}$; negative samples: $\{32, 64\}$; aggregation function: sum, PNA (Principal Neighborhood Aggregator [4]; number of hidden layers: $\{4, 5, 6\}$; hidden layer dimension: $\{32, 64\}$; learning rate $\{5e-3, 1e-3, 5e-4\}$. Optimal

hyperparameter set of BioPathNet {'layers': 6, 'hidden_dim': 32, 'num_negatives': 32, 'lr': 0.005, 'adversarial_temperature': 0.5, 'batch_size': 8, 'epochs': 8}. Hyperparameters were optimized on the validation MRR.

1.3 Drug repurposing task

For this task, the hyperparameter search for the BioPathNet model considered the parameters dependent $= \{yes, no\}$, number of hidden layers $= \{2, 4, 6, 8\}$, aggregator function $= \{sum, pna\}$, adversarial temperature $= \{0.5, 1, 2, 5\}$, and number of negative samples $= \{32, 64, 128\}$. The best MRR performance in the KG completion validation set determined the final parameter set. The experiments were repeated for five different data split seeds in the TxGNN code. The mean $\pm$ standard deviation of performance metrics were reported.

1.4 Synthetic lethality gene pair prediction task

We train BioPathNet for 15 epochs and for five random seeds and tuned hyperparameters such as the number of hidden layers in $\{4, 5\}$, the number of sampled negatives per positive example in $\{32, 64\}$, and the adversarial temperature in $\{0.5, 1.0, 2.0, 5.0\}$. Optimal hyperparameter set of BioPathNet {'layers': 5, 'hidden_dim': 32, 'num_negatives': 64, 'lr': 0.005, 'adversarial_temperature': 0.5, 'batch_size': 64, 'epochs': 15}.

1.5 LncRNA-target prediction task

The KG constructed by LncTarD 2.0 consists mainly of a densely connected subgraph of 2,646 genes and 6,084 involved regulations, surrounded by many isolated subgraphs containing only two or three genes. Only the largest connected component was kept and split into train, validation, and test set using the python package PyKeen [5], at a ratio of 0.8, 0.1, and 0.1, while ensuring that all nodes were included in the training set with at least one triplet. The optimal hyperparameter set of BioPathNet in this setting was: {'layers': 6, 'hidden_dim': 32, 'num_negatives': 32, 'lr': 0.005, 'adversarial_temperature': 0.5, 'batch_size': 64, 'epochs': 10}.

1.6 Baseline methods used for comparison

TransE The key idea of TransE is to model relationships as translations in the embedding space. For each triplet (u, r, v), the relationship r is modeled as a translation vector such that the embedding of the tail entity v should be close to the embedding of the head entity u plus the embedding of the relationship r: $\mathbf{u} + \mathbf{r} \approx \mathbf{v}$. The plausibility of a triplet (u, r, v) is determined by a scoring function based on the distance between $\mathbf{u} + \mathbf{r}$ and v: $f(u, r, v) = \|\mathbf{u} + \mathbf{r} - \mathbf{v}\|_2$. TransE is trained to minimize the distance for correct triplets and maximize the distance for incorrect triplets using a margin-based ranking loss [6]. The following hyperparameters were used: {'embedding_dim': 512, 'num_negatives': 512, 'lr': 0.0005, 'epochs': 100}. The code for training is an efficient re-implemtnation of the original algorithm and can be found at the following link: https://github.com/DeepGraphLearning/torchdrug (inside /torchdrug/models/embedding.py)

RotatE RotatE is a KGE model that represents entities as complex-valued vectors and relationships as rotations in the complex plane. This allows the model to capture various relational patterns, including symmetry, antisymmetry, inversion, and composition. Each entity u and v (head and tail) is represented as a complex vector, and each relationship r is represented as a complex vector with a modulus of 1, representing a rotation in the complex plane. For a triplet (u, r, v), the relationship r rotated u to match v, $v \approx u \circ v$, where $\circ$ denotes the element-wise (Hadamard) product. The plausibility of a triplet (u, r, v) is determined by a scoring function based on the distance between u and v: $f(u, r, v) = \|\mathbf{u} \circ \mathbf{r} - \mathbf{v}\|_2$. RotatE is trained to minimize the distance for correct triplets and maximize the distance for incorrect triplets using a margin-based ranking loss [7]. The following hyperparameters

were used: {'embedding_dim': 512, 'num_negatives': 512, 'lr': 0.0005, 'epochs': 100}. The code for training is an efficient re-implemtnation of the original algorithm and can be found at the following link: https://github.com/DeepGraphLearning/torchdrug (inside /torchdrug/models/embedding.py)

DistMult DistMult (Multiplicative Distance) is a knowledge graph embedding model that represents entities and relationships as vectors and captures interactions through a multiplicative mechanism. Each entity u and v (head and tail) and each relationship r is represented as a vector in the embedding space. For a triplet (u, r, v), the relationship r interacts multiplicatively with the head entity u to predict the tail entity v: $v \approx u \circ r$, where $\circ$ denotes the element-wise (Hadamard) product. The plausibility of a triplet (u, r, v) is determined by a scoring function that measures the similarity between $u \circ r$ and v: $f(u, r, v) = -\|\mathbf{u} \circ \mathbf{r} - \mathbf{v}\|_2^2$. DistMult is trained to maximize the score for correct triplets and minimize the score for incorrect triplets using, similarly to TransE, a margin-based ranking loss [8]. The following hyperparameters were used: {'embedding_dim': 512, 'num_negatives': 512, 'lr': 0.001, 'L_3 regularization' = 1e-4, 'epochs': 100}. The code for training is an efficient re-implemtnation of the original algorithm and can be found at the following link: https://github.com/DeepGraphLearning/torchdrug (inside /torchdrug/models/embedding.py)

Relational Graph Convolutional Networks (R-GCNs) R-GCN is a variant of the Graph Convolutional Network (GCN) specifically designed to handle graphs with multiple types of relations. R-GCN extends GCN to incorporate relational data, making it suitable for KGs. R-GCN employs a neural encoder to learn the representation for each node, while the decoder retains the scoring functions from the KGE models. Initially, the embeddings for each node are initialized [9]. During each layer of the GNN's message passing, messages are passed, aggregated, and used to update the node's embedding. The messages are obtained by applying a $W_{r,M}^{(l)}$ matrix on the embeddings of the previous layer $h_i^{(l-1)}$ separately for each relation r, allowing R-GCN to handle graphs with multiple types of edges by learning separate weight matrices for each relation type: $m_{r,i}^{(l)} = W_{r,M}^{(l)} h_i^{(l-1)}$. Next, the incoming messages of each node v_i from the neighboring nodes $N_r(i)$ are aggregated by the taking the average: $\widetilde{m_{r,i}^{(l)}} = \frac{1}{|N_r(l)|} \sum_{j \in N_r(i)} m_{r,j}^{(l)}$. Finally, the node's embedding from the previous layer is updated by $h_i^{(l)} = h_i^{(l-1)} + \sum_{r \in T_R} \widetilde{m_{r,i}^{(l)}}$. This process ensures that each node's embedding is updated with information from its neighbors, considering the type of relation connecting them. The final embeddings of the nodes are derived after L layers of propagation. The hyperparameters for R-GCN were optimized using grid search on the parameters *num_negatives*, *lr* and *hidden_dim*. Two separate searches were conducted: one without the BRG, yielding the best set as {'num_negatives': 64, 'lr': 10^{-4}, 'layers': 3, 'hidden_dim' = 256}, and another with the BRG, resulting in the best set as {'num_negatives': 32, 'lr': 10^{-5}, 'layers': 5, 'hidden_dim' = 128}. The code for training is an efficient re-implemtnation of the original algorithm and can be found at the following link: https://github.com/DeepGraphLearning/torchdrug (inside /torchdrug/models/gcn.py)

Transductive Graph Neural Network (TxGNN) TxGNN is a graph neural network-based model designed to predict drug-disease relationships in zero-shot scenarios where there is minimal prior information or treatment history. Utilizing PrimeKG, a comprehensive biomedical knowledge graph, TxGNN employs R-GCNs to learn embeddings of drugs and diseases, capturing complex interactions by mapping them into a shared latent space. This allows TxGNN to predict drug-disease interactions, focusing on indications and contraindications, even for diseases with limited molecular characterization. It achieves this through the use of disease signature vectors, adaptive embedding aggregation, and iterative optimization of non-linear transformations. TxGNN improves drug-disease prediction by splitting training into pre-training and fine-tuning phases. In pre-training, all triplets are used, while fine-tuning focuses on drug-disease relations like `indication`, `contraindications`, and `off-label use`. This is in contrast to BioPathNet, where we do not divide our approach into these two phases or perform pre-training. Instead, we use all triplets containing non-drug-disease relations in the message passing BRG without considering them for supervision. TxGNN was trained using the hyperparameters provided in the original publication: pretraining: {'lr': $1e-3$, 'batch_size': 1024, 'pretrain epochs': 2}; finetuning: {'lr': $5e-4$, 'hidden_dim': 512, 'batch_size': 1024, 'pretrain epochs': 500}. The hyperparameters

used in fine-tuning were the same for all disease splits. The code used for trinaing can be found here: https://github.com/mims-harvard/TxGNN

Knowledge Representation for Synthetic Lethality (KR4SL) KR4SL is a path-representation learning GNN-based method for the prediction of SL gene pairs. The framework begins with the construction of a heterogeneous KG that integrates genes, gene interactions, pathways, GO terms, and an SL graph augmented with reverse and identity edges. This graph is processed through an encoder that identifies relevant relational paths for each primary gene, combining structural graph information with textual semantics of entities. KR4SL utilizes a gated recurrent unit (GRU) to enhance the sequential semantics of the relational paths. As messages propagate through the network, they are enriched by fusing structural and textual information. An attentive aggregation mechanism evaluates the importance of different edges, focusing on the most essential paths for model explanations. Finally, a scoring decoder processes the semantic representations of candidate SL partners, generating scores to rank and select the top-k candidates as the most probable SL partners. The code used for trinaing can be found here: https://github.com/JieZheng-ShanghaiTech/KR4SL.

We use the code from GitHub to train KR4SL in the transductive setting. We trained KR4SL on the original (unthresholded) data using the same hyperparameters specified by the authors on GitHub, 'weight decay rate': 0.000089, 'lr': 0.0011, 'batch_size': 50, 'epochs': 15, 'hidden_dim': 48, 'drop_out': 0}. The experiments were run five times with different seeds. The same set of parameters was used for thresholded data.

1.7 Model Evaluation

Models were evaluated by ranking positive triplets $\langle u, r, v\rangle$ of the test set against all negative triplets $\langle u, r, v'\rangle$ that are not present in the KG, following the filtered ranking protocol [8]. Equally, for the reverse relation direction r^{-1}, positive triplets of the form $\langle v, r, u\rangle$ are ranked against all negatives $\langle v, r^{-1}, u\rangle$. This approach yields a very stringent evaluation that forces the model to rank positive samples highly. The metrics used are mean rank (MR), mean reciprocal rank (MRR), and hits at k (Hits@k). MR is calculated by averaging the ranks q of the positive samples among negatives. Lower values are ideal, with the best value at 1.

$$MR = \frac{1}{|Q|}\sum_{q\in Q} q \tag{10}$$

MRR is the average of the reciprocal rank $\frac{1}{q}$, placing less emphasis on lowly ranked triplets. The values range in $[0, 1]$, and the larger the value, the better the model.

$$MRR = \frac{1}{|Q|}\sum_{q\in Q} \frac{1}{q} \tag{11}$$

Finally, the metric Hits@k provides the probability of correct predictions in the top k predicted triplets made by the model. It can also be considered the percentage of positive triplets in the top k and is, therefore, equivalent to Recall@k. Like MRR, values range in $[0, 1]$, and the larger the value, the better the model.

$$H@k = \frac{\big|\{q \in Q : q < k\}\big|}{\big|Q\big|} \tag{12}$$

The best model is selected based on the highest MRR in a validation set.

While the conditional probability is modeled in KGC by predicting the tail entity v given the head entity u and the relation r, it might be sensible to evaluate under the joint probability of u, v, and r. Therefore, to remain consistent with the TxGNN we compared against in the drug prediction task, we also used AUPRC, which summarizes the precision and recall at different probability thresholds, as well as specificity and F1 score at the probability threshold of 0.5 (equation 13) using code inherent to TxGNN. They evaluate the performance per disease node.

$$Precision = \frac{TP}{TP + FP},\ Recall = \frac{TP}{TP + FN},\ F1 = 2 \times \frac{Precision \times Recall}{Precision + Recall} \tag{13}$$

TxGNN calculates AUPRC using two strategies. The first compares each positive ground truth item vs. one negative from the list of drugs of a disease area, referred to as `AUPRC 1:1`. The second considers all positive and negative ground truth items, referred to as `AUPRC`. The first metric conveys information on the model's ability to distinguish a positive from a randomly sampled negative in direct comparison. In contrast, the latter focuses on distinguishing positives and negatives across the whole dataset. Furthermore, the `AUPRC` accounts for the positive/negative class imbalance and provides a balanced evaluation of precision and recall. We chose to predominately use the latter, which reflects a real-world scenario of identifying therapeutical opportunities within a given set of drugs.

For the SL prediction task, we compared the seed-wise performance of our model with the performance of KR4SL using metrics inherent to the KR4SL framework's code: NDCG@k, Recall@k, and Precision@k. Moreover, we computed MRR from equation 11 for both BioPathNet and KR4SL by first calculating MRR for each query gene and then averaging gene-wise MRR overall query genes.

Recall@k here is utilized to evaluate how effectively a model predicts SL relationships within its top k predictions and is defined as follows:

$$Recall@k = \frac{1}{N} \sum_{n=1}^{N} \frac{\sum_{i=1}^{k} \mathbb{1}\{G_n^{KR}(i) \in G_n^{KP}\}}{|G_n^{KP}|} \tag{14}$$

where N is the total number of query genes, G_n^{KP} is the set of known SL partner candidates of gene n and G_n^{KR} is the set of top-k SL gene partners for gene n ranked by prediction scores meaning that $G_n^{KR}(i)$ is i-th predicted SL partner for gene n.

Respectively, Precision@k is employed to assess how effectively a model predicts SL relationships within its top-k predictions, normalized by either the size of the top-k predictions or the size of the known SL relationships, whichever is smaller. Precision@k is defined as follows:

$$Precision@k = \frac{1}{N} \sum_{n=1}^{N} \frac{\sum_{i=1}^{k} \mathbb{1}\{G_n^{KR}(i) \in G_n^{KP}\}}{min\{|G_n^{KP}|, k\}} \tag{15}$$

NDCG@k is used to evaluate a model's capability to prioritize the top-k candidate genes associated with SL relationships and is defined as follows:

$$NDCG@k = \frac{1}{N} \sum_{n=1}^{N} \frac{DCG@k(n)}{IDCG@k(n)} \tag{16}$$

where $DCG@k(n)$ and $IDCG@k(n)$ are defined as follows:

$$DCG@k(n) = \sum_{i=1}^{k} \frac{2^{\mathbb{1}\{G_n^{KR}(i) \in G_n^{KP}\}} - 1}{log_2(i+1)} \tag{17}$$

$$IDCG@k(n) = \sum_{i=1}^{min\{|G_n^{KP}|, k\}} \frac{1}{log_2(i+1)} \tag{18}$$

2 Supplementary Tables

2.1 Gene function prediction task

Supplementary Table 1: Summary of the dataset for the gene function prediction task: the **number of nodes, edges and relation types** in the background regulatory graph (BRG) obtained from Pathway Commons, as well as train, validation and test set obtained from KEGG.

	Number of nodes	Number of edges	Number of relations
BRG	30,885	1,884,146	13
Train	7,070	22,702	1
Valid	2,348	3,243	1
Test	3,533	6,487	1
Unique count	31,410	1,916,513	14

Supplementary Table 2: Detailed breakdown of the relation types in the functional annotation data set: **Number of edges per relation type** in BRG, train, validation and test set.

	Relation	Count
BRG	controls-transport-of-chemical	3,741
	reacts-with	4,063
	controls-transport-of	7,899
	used-to-produce	14,747
	controls-phosphorylation-of	17,660
	controls-production-of	21,262
	consumption-controlled-by	22,659
	controls-expression-of	125,860
	catalysis-precedes	147,948
	in-complex-with	191,275
	controls-state-change-of	191,548
	interacts-with	517,390
	chemical-affects	618,094
Train	KEGGPathway	22,702
Valid	KEGGPathway	3,227
Test	KEGGPathway	6,438

Supplementary Table 3: **Best hyperparameter sets for gene function prediction tasks** with and without BRG, *dim* refers to embedding dimension, L is the number of hidden layers, *lr* is the learning rate, *Adv. T* the adversarial temperature used in self-adversarial negative sampling, *Aggr. Function* specifies the aggregation function, relevant only for BioPathNet that can choose between *sum* and *PNA*.

Model	*dim*	*L*	*lr*	*NegSam*	*Adv. T*	*Aggr. Function*
TransE w BRG	128	-	1e-3	512	1	-
TransE w/o BRG	512	-	5e-4	512	1	-
DistMult w BRG	128	-	1e-3	512	1	-
DistMult w/o BRG	512	-	1e-3	512	1	-
RotatE w BRG	128	-	2e-4	512	1	-
RotatE w/o BRG	512	-	5e-4	512	1	-
R-GCN w BRG	128	5	5e-4	32	1	-
R-GCN w/o BRG	256	3	1e-4	64	1	-
BioPathNet w BRG	32	6	5e-3	32	1	PNA
BioPathNet w/o BRG	32	6	5e-3	32	1	PNA

2.2 Drug repurposing task

Supplementary Table 4: **Number of diseases per disease area split**, as well as the number of edges used as BRG and for training, validation, and testing.

Disease area	Number of diseases	BRG	Train	Valid	Test contraindication	Test indication
Adrenal gland	6	5,728,452	33,063	4,723	303	33
Anemia	19	5,705,775	33,715	4,817	752	88
Cardiovascular	111	5,695,332	30,930	4,419	4,215	453
Cell proliferation	201	5,689,920	33,102	4,729	1,047	999
Mental health	60	5,690,512	33,443	4,778	1,567	355

Supplementary Table 5: **Zero-shot prediction scenario for Alzheimer's disease**: diseases included and number of contraindication and indication drugs in custom data split generated following TxGNN code on disease evaluation.

Disease	ID	# contraindication	# indication
Alzheimer disease	28,780	56	8
Alzheimer disease w/o neurofibrillary tangles	83,960	2	7
Lewy body dementia	29,296	2	0
Pick disease	28,473	27	7
Dementia (disease)	37,573	28	3

Supplementary Table 6: **Best Hyperparameter Sets for Each Disease Area Split**, *dim* refers to embedding dimension, L is the number of hidden layers, lr is the learning rate, $Adv.\ T$ the adversarial temperature used in self-adversarial negative sampling, *Aggr. Function* specifies the aggregation function, in this case PNA was always the best performing.

Disease Area	*dim*	*L*	*lr*	*NegSam*	*Adv. T*	*Aggr. Function*
Adrenal Gland	32	6	5e-3	64	0.5	PNA
Anemia	32	4	1e-3	64	1.0	PNA
Cardiovascular	32	6	1e-3	64	0.5	PNA
Cell Proliferation	32	6	1e-3	64	1.0	PNA
Mental Health	32	4	5e-3	64	1.0	PNA
Alzheimer	32	6	5e-3	64	1.0	PNA

Supplementary Table 7: **Performances across five different disease area splits**, mean metrics summarized as average across contraindication and indication.

Anemia

	Recall @20	AP @20	MRR @20	F1	AUPRC 1:1	AUPRC
TxGNN	0.45	0.457	0.535	0.244	0.667	0.352
BioPathNet	**0.504**	**0.493**	**0.52**	**0.305**	**0.674**	**0.412**

Adrenal gland

	Recall @20	AP @20	MRR @20	F1	AUPRC 1:1	AUPRC
TxGNN	**0.604**	0.724	0.725	**0.612**	0.587	0.632
BioPathNet	0.562	**0.903**	**0.9**	0.405	**0.582**	**0.721**

Cardiovascular

	Recall @20	AP @20	MRR @20	F1	AUPRC 1:1	AUPRC
TxGNN	0.1	0.17	0.199	0.059	0.606	0.108
BioPathNet	**0.166**	**0.23**	**0.249**	**0.074**	**0.605**	**0.136**

Cell proliferation

	Recall @20	AP @20	MRR @20	F1	AUPRC 1:1	AUPRC
TxGNN	0.539	0.487	0.549	0.256	0.811	0.437
BioPathNet	**0.604**	**0.626**	**0.654**	**0.404**	**0.813**	**0.556**

Mental health

	Recall @20	AP @20	MRR @20	F1	AUPRC 1:1	AUPRC
TxGNN	0.167	0.228	0.264	0.112	0.617	0.16
BioPathNet	**0.219**	**0.265**	**0.297**	**0.132**	**0.57**	**0.187**

2.3 Synthetic lethality gene pair prediction task

Supplementary Table 8: **The statistics** of the BRG and SL graph as reported by KR4SL.

	# Entities	# Relationss	# Triples
SL graph	9,746	1	35,374
BRG	42,547	32	381,761

Supplementary Table 9: **Number of edges and source genes** in each data split for various thresholds

threshold	0.0	0.2	0.3	0.4	0.5	0.6	0.7	0.8
# edges (BRG)	396,619	396,221	394,922	392,429	390,151	386,705	385,090	384,900
# genes (BRG)	14,858	14,460	13,161	10,668	8,390	4,944	3,329	3,139
# edges (train)	9,878	9,617	8,770	7,038	5,540	3,274	2,137	2,015
# genes (train)	5,444	5,363	4,747	3,252	2,597	1,804	846	755
# edges (valid)	3,533	3,447	3,172	2,568	2,004	1,184	764	721
# genes (valid)	2,918	2,870	2,544	1,803	1,412	946	556	516
# edges (test)	7,049	6,887	6,254	5,029	3,909	2,279	1,556	1,466
# genes (test)	4,474	4,407	3,853	2,601	2,020	1,367	739	664

Supplementary Table 10: **Detailed breakdown of the relation types** in the SynLethDB: Number of edges per head and tail type in BRG

Entity 1	Relation	Entity 2	# Triples
gene	participates GpPW	Pathway	41,726
gene	NOT|enables	molecular function	233
gene	NOT|involved in	biological process	376
gene	NOT|is active in	cellular component	3
gene	NOT|located in	cellular component	109
gene	NOT|part of	cellular component	134
gene	is active in	cellular component	8,749
gene	located in	cellular component	51,382
gene	part of	cellular component	60,679
gene	acts upstream of or within	biological process	202
gene	acts upstream of	biological process	158
gene	acts upstream of negative effect	biological process	2
gene	acts upstream of or within negative effect	biological process	2
gene	acts upstream of or within positive effect	biological process	7
gene	acts upstream of positive effect	biological process	15
gene	colocalizes with	cellular component	874
gene	contributes to	molecular function	752
gene	enables	molecular function	54,511
gene	involved in	biological process	105,623
gene	NOT|colocalizes with	cellular component	9
gene	NOT|contributes to	molecular function	3
gene	NOT|acts upstream of or within	biological process	1
gene	NOT|acts upstream of or within negative effect	biological process	1
biological process	happens during	biological process	7
biological process	has part	biological process	144
biological process	has part	molecular function	94
biological process	is a	biological process	33158
biological process	negatively regulates	biological process	1,858
biological process	negatively regulates	molecular function	192
biological process	occurs in	cellular component	119
biological process	part of	biological process	3,144
biological process	positively regulates	biological process	1,834
biological process	positively regulates	molecular function	200
biological process	regulates	biological process	2,092
biological process	regulates	molecular function	218
cellular component	has part	cellular component	154
cellular component	is a	cellular component	3,224
cellular component	part of	cellular component	1,222
molecular function	has part	molecular function	167
molecular function	is a	molecular function	7,493
molecular function	negatively regulates	molecular function	50
molecular function	occurs in	cellular component	31
molecular function	part of	biological process	722
molecular function	part of	molecular function	8
molecular function	part of	Pathway	1
molecular function	positively regulates	molecular function	40
molecular function	regulates	biological process	1
molecular function	regulates	molecular function	36

Supplementary Table 11: **Best hyperparameter set for Synthetic lethality gene pair prediction task**, *dim* refers to embedding dimension, L is the number of hidden layers, lr is the learning rate, *Adv.* T the adversarial temperature used in self-adversarial negative sampling, *Aggr. Function* specifies the aggregation function.

Model	*dim*	*L*	*lr*	*NegSam*	*Adv. T*	*Aggr. Function*
BioPathNet	32	5	5e-3	64	0.5	PNA

Supplementary Table 12: **Performance comparison between BioPathNet and state-of-the-art** SL gene pair prediction method KR4SL for **unthresholded data**.

	seed 1234		seed 1235		seed 1236		seed 1237		seed 1238	
metric	KR4SL	BioPathNet	KR4SL	BioPathNet	KR4SL	BioPathNet	KR4SL	BioPathNet	KR4SL	BioPathNet
MRR	0.285	0.295	0.284	0.300	0.285	0.297	0.280	0.294	0.284	0.299
NDCG@10	0.341	0.364	0.341	0.362	0.343	0.360	0.337	0.366	0.340	0.366
NDCG@20	0.356	0.383	0.355	0.381	0.357	0.378	0.352	0.383	0.354	0.384
NDCG@50	0.368	0.400	0.368	0.397	0.369	0.394	0.364	0.400	0.367	0.401
Precision@10	0.434	0.451	0.439	0.455	0.437	0.450	0.435	0.452	0.437	0.455
Precision@20	0.485	0.515	0.484	0.519	0.486	0.511	0.484	0.511	0.485	0.516
Precision@50	0.529	0.580	0.533	0.581	0.532	0.572	0.530	0.574	0.533	0.580
Recall@10	0.424	0.440	0.428	0.444	0.427	0.440	0.424	0.441	0.426	0.444
Recall@20	0.480	0.511	0.480	0.515	0.482	0.507	0.479	0.507	0.481	0.512
Recall@50	0.528	0.579	0.532	0.580	0.531	0.571	0.529	0.573	0.532	0.579

Supplementary Table 13: **Performance comparison between BioPathNet and state-of-the-art** SL gene pair prediction method KR4SL for **thresholded data**.

	seed 1234		seed 1235		seed 1236		seed 1237		seed 1238	
metric	KR4SL	BioPathNet	KR4SL	BioPathNet	KR4SL	BioPathNet	KR4SL	BioPathNet	KR4SL	BioPathNet
MRR	0.338	0.360	0.339	0.360	0.336	0.348	0.333	0.362	0.339	0.353
NDCG@10	0.398	0.420	0.401	0.416	0.399	0.406	0.396	0.418	0.401	0.412
NDCG@20	0.416	0.437	0.415	0.434	0.415	0.427	0.412	0.436	0.416	0.432
NDCG@50	0.428	0.453	0.428	0.451	0.428	0.443	0.425	0.452	0.429	0.448
Precision@10	0.507	0.525	0.512	0.519	0.513	0.508	0.511	0.519	0.513	0.517
Precision@20	0.569	0.583	0.560	0.581	0.570	0.579	0.566	0.581	0.565	0.584
Precision@50	0.611	0.641	0.608	0.644	0.615	0.641	0.613	0.638	0.612	0.642
Recall@10	0.496	0.514	0.501	0.508	0.501	0.498	0.499	0.507	0.501	0.506
Recall@20	0.564	0.579	0.556	0.577	0.566	0.575	0.562	0.576	0.561	0.580
Recall@50	0.610	0.640	0.608	0.643	0.614	0.640	0.612	0.637	0.611	0.641

2.4 LncRNA-gene target prediction task

Supplementary Table 14: Summary of the functional annotation data set: **number of nodes, edges and relation types** in the background regulatory graph (BRG), as well as train, validation and test sets.

	Number of nodes	Number of edges	Number of relations
BRG	15,806	1,035,133	7
Train	2,646	4,867	6
Valid	533	608	6
Test	535	609	6
Unique count	16,844	1,041,217	13

Supplementary Table 15: Detailed breakdown of the relation types in the functional annotation data set: **Number of edges per relation type** in BRG, train, validation and test set.

	Relation	Count
BRG	interacts-with	469,203
	in-complex-with	154,868
	controls-state-change-of	144,259
	catalysis-precedes	141,554
	controls-expression-of	114,698
	controls-phosphorylation-of	7,246
	controls-transport-of	3,305
Train	ceRNA or sponge	2,305
	expression association	1,530
	interact with protein	366
	transcriptional regulation	351
	epigenetic regulation	272
	interact with mRNA	43
Valid	ceRNA or sponge	275
	expression association	208
	interact with protein	48
	transcriptional regulation	44
	epigenetic regulation	31
	interact with mRNA	2
Test	ceRNA or sponge	247
	expression association	228
	interact with protein	52
	transcriptional regulation	47
	epigenetic regulation	28
	interact with mRNA	7

Supplementary Table 16: **Best hyperparameter set for LncRNA-gene target prediction task**, *dim* refers to embedding dimension, L is the number of hidden layers, *lr* is the learning rate, *Adv. T* the adversarial temperature used in self-adversarial negative sampling, *Aggr. Function* specifies the aggregation function.

Model	*dim*	*L*	*lr*	*NegSam*	*Adv. T*	*Aggr. Function*
BioPathNet	32	6	5e-3	64	0.5	PNA

3 Supplementary Figures

3.1 Supplementary Figure 1

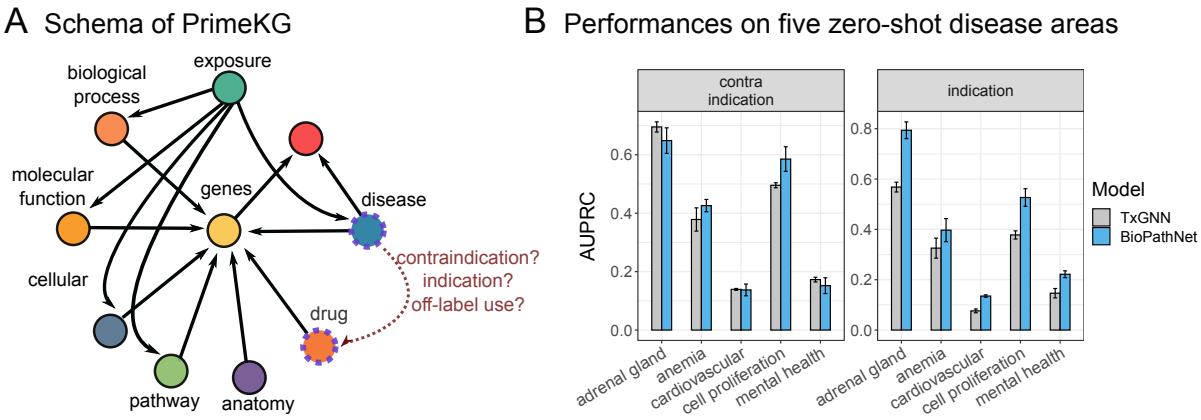

Supplementary Figure 1: **BioPathNet's performance on PrimeKG A**) PrimeKG schema: a multi-modal knowledge graph with 10 biological node types (e.g., protein, disease, drug) and over 5 million relations, for predicting drug-disease interactions. **B**) AUPRC performance in zero-shot prediction across five disease area splits (adrenal gland, anemia, cardiovascular, cell proliferation, mental health), calculated by comparing ground truth positives and negatives, then averaging across all diseases in each area.

3.2 Supplementary Figure 2

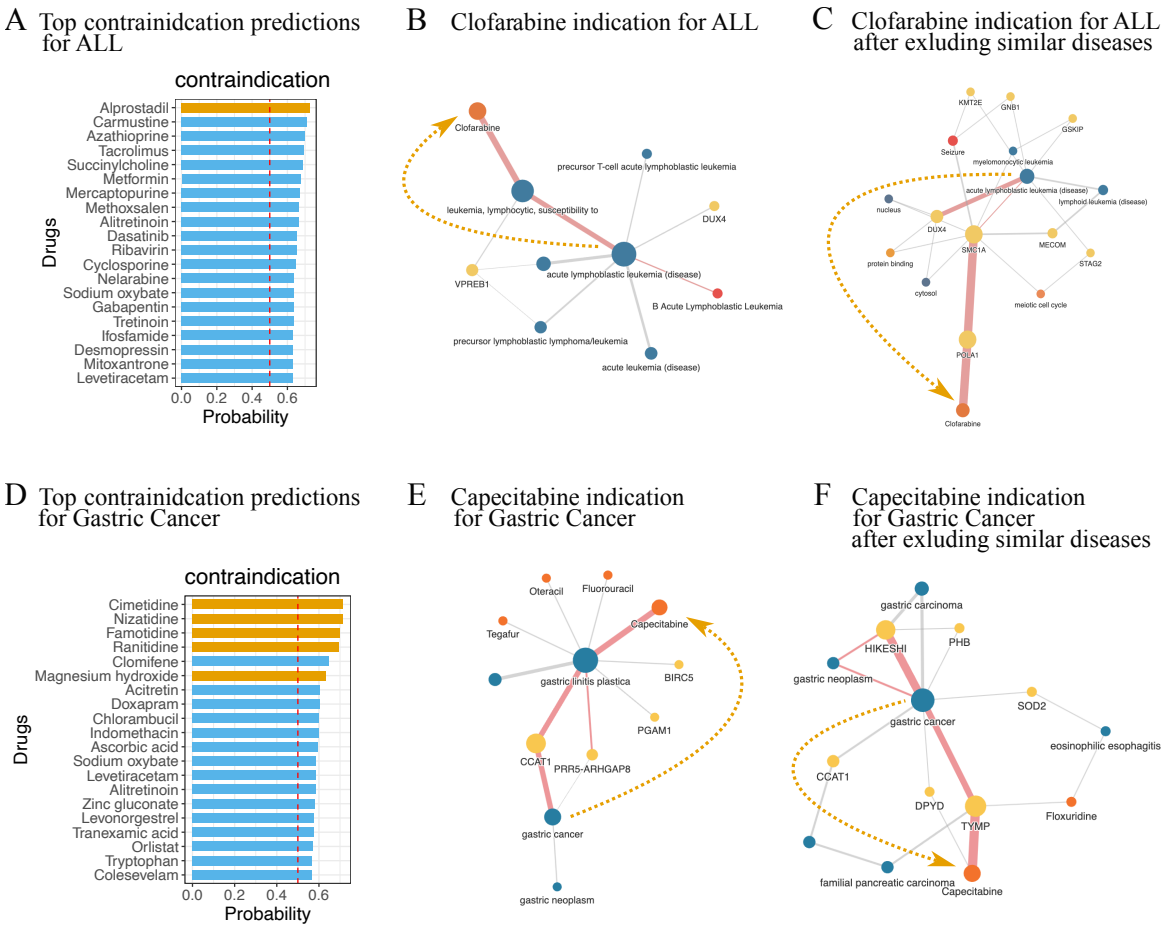

Supplementary Figure 2: **Inspecting BioPathNet predictions in zero-shot learning A**) Top 20 predictions of contraindication for ALL. Path interpretation for the prediction of Clorafabine as an indication for ALL in near-shot learning scenario (**B**) and in zero-shot scenario (**C**). **D**) Top 20 predictions of contraindication for Gastric Cancer. Path interpretation for the prediction of Capecitabine as an indication for Gastric Cancer in near-shot learning scenario (**E**) and in zero-shot scenario (**F**). Known contraindications, included in the ground truth of PrimeKG, are highlighted in orange, while while newly predicted contraindications are in light blue. The visualization (B-C and E-F) shows the top 10 significant paths used by BioPathNet for prediction, with edge widths representing weights and the highest-weight path highlighted in red.

3.3 Supplementary Figure 3

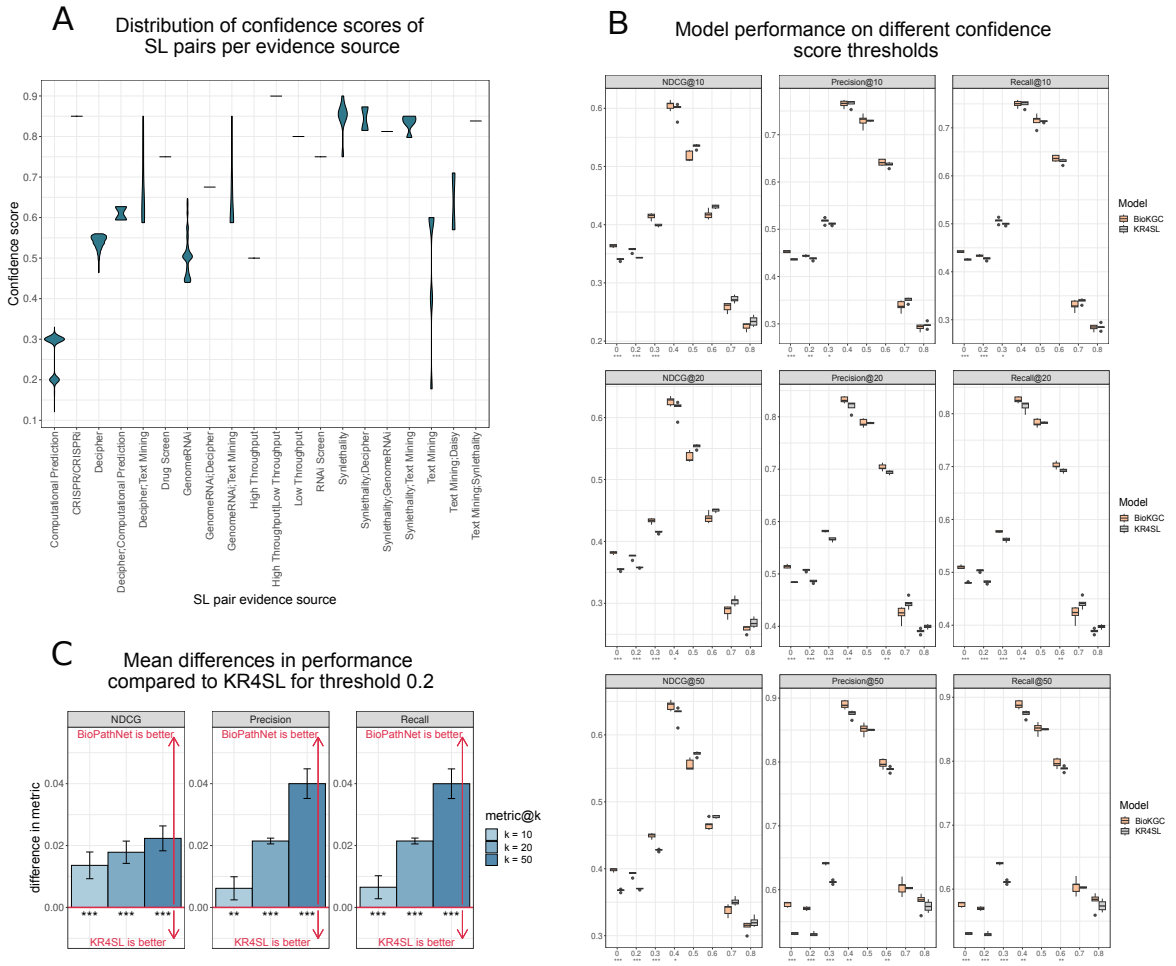

Supplementary Figure 3: **Comparison of BioPathNet with state-of-the-art SL gene pair prediction algorithm KR4SL for varying SL confidence thresholds: A**) Distribution of confidence scores of SL pairs per evidence source as provided by SynLethDB-v2.0 as the "r.statistic_score". **B**) Performance comparison of BioPathNet and KR4SL with performance metrics reported across thresholds applied to the confidence score of SL evidence. **C**) Difference in performances between BioPathNet and KR4SL for both methods trained on SL pairs which were filtered to have a confidence score of at least 0.2. Bars are shown for each metric (NDCG, Precision, Recall) and different k, and represent the mean difference in performance, while error bars denote standard deviations for the different seeds ($N = 5$). BioPathNet significantly outperformed KR4SL on 0.2-thresholded data (p-values: $p = 1.07 \times 10^{-3}$, $p = 1.89 \times 10^{-4}$, $p = 1.21 \times 10^{-4}$ for NDCG@k; $p = 1.04 \times 10^{-2}$, $p = 4.19 \times 10^{-7}$, $p = 2.42 \times 10^{-5}$ for Precision@k; and $p = 8.57 \times 10^{-3}$, $p = 4.59 \times 10^{-7}$, $p = 2.43 \times 10^{-5}$ for Recall@k, for $k \in \{10, 20, 50\}$.)

3.4 Supplementary Figure 4

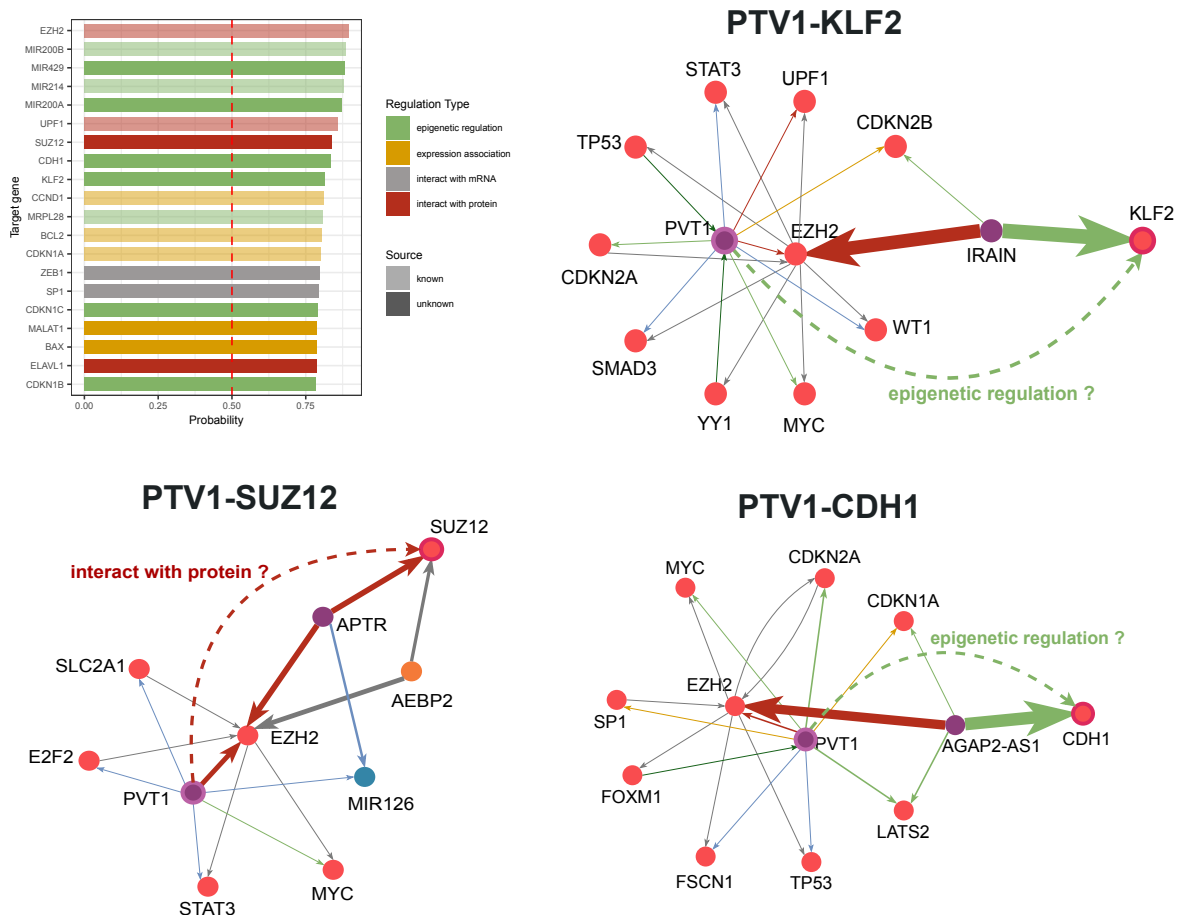

Supplementary Figure 4: **Prediction of novel incRNA-target regulatory interactions. A** presents BioPathNet predicted targets for the cancer lncRNA PVT1, ranked by prediction probability, similar to Figure 6A. Additionally, regulation types are distinguished using different colors: green for epigenetic regulation, yellow for expression association, gray for interaction with mRNA, and red for interaction with protein. Known triples are shown with 50% transparency, while novel triples are displayed with full opacity. **B-D** Explanations for top 3-5 novel predicted targets of PVT1: SUZ12, CDH1, and KLF2.

References

[1] Bang-Jensen, J., Gutin, G.: Section 2.3.4: The Bellman-Ford-Moore algorithm. Digraphs: Theory, Algorithms and Applications. Springer, London (2000)

[2] Baras, J.S., Theodorakopoulos, G.: Path problems in networks. Synth. Lect. Commun. Netw. **3**(1), 1–77 (2010)

[3] Zhu, Z., Zhang, Z., Xhonneux, L.-P., Tang, J.: Neural bellman-ford networks: A general graph neural network framework for link prediction. In: Advances in Neural Information Processing Systems, vol. 34, pp. 29476–29490. Curran Associates Inc., Virtual Event (2021)

[4] Corso, G., Cavalleri, L., Beaini, D., Liò, P., Veličković, P.: Principal neighbourhood aggregation for graph nets. Preprint at http://arxiv.org/abs/2004.05718 (2016)

[5] Pykeen/Pykeen. PyKEEN

[6] Nguyen, P.H., *et al.*: All-trans retinoic acid targets gastric cancer stem cells and inhibits patient-derived gastric carcinoma tumor growth. Oncogene **35**(43), 5619–5628 (2016)

[7] Sun, Z., Deng, Z.-H., Nie, J.-Y., Tang, J.: Rotate: Knowledge graph embedding by relational rotation in complex space. In: International Conference on Learning Representations (2019)

[8] Bordes, A., Usunier, N., Garcia-Duran, A., Weston, J., Yakhnenko, O.: Translating embeddings for modeling multi-relational data. In: Advances in Neural Information Processing Systems, vol. 26. Curran Associates Inc., Harrahs and Harveys, Lake Tahoe (2013)

[9] Glorot, X., Bengio, Y.: Understanding the difficulty of training deep feedforward neural networks. In: Teh, Y.W., Titterington, M. (eds.) Proceedings of the 13th International Conference on Artificial Intelligence and Statistics, pp. 249–256. PMLR, Chia Laguna Resort, Sardinia, Italy (2010)